ASTRONOMY & ASTROPHYSICS
SUPPLEMENT SERIES

Astron. Astrophys. Suppl. Ser. **55**, 171-177 (1984)

Clean lines in the solar flux spectrum

R. J. Rutten and E. B. J. van der Zalm

Sterrewacht « Sonnenborgh », Zonnenburg 2, 3512 NL Utrecht, The Netherlands

Received July 19, accepted October 12, 1983

Summary. — We list profile parameters of 602 unblended lines in the Sacramento Peak Atlas of the visual solar irradiance spectrum, and we compare these to our earlier measurements of the same lines in the Jungfraujoch Atlas of the solar disk-center intensity spectrum.

Key words : solar spectroscopy — stellar abundances.

1. Introduction.

In our previous paper (Rutten and van der Zalm, 1984; henceforth paper I) we have selected 750 unblended lines present in the visual disk-center spectrum of the sun, and provide a list of various line-profile parameters. In this paper we extend these solar clean-line data by adding profile parameters measured from the full-disk spectrum. We so make an intermediate step between solar resolved-disk intensity spectrometry and stellar full-disk flux spectrometry; the list compiled here should be useful for stellar abundance analysis.

Paper I is based on the Jungfraujoch Atlas of the visual disk-center spectrum (Delbouille *et al.*, 1973; henceforth JJ Atlas). Here we use the Sacramento Peak Irradiance Atlas of the full-disk spectrum (Beckers *et al.*, 1976; henceforth SP Atlas). Each atlas has been recorded photoelectrically with a double-pass scanning-grating spectrometer, and each furnishes the highest spectral purity (spectral resolution, signal-to-noise ratio, absence of distortion) available for the respective spectrum. For our purposes their instrumental broadening is negligible; while the resolution of the SP Atlas is somewhat coarser, so is the inherent spectral detail of the flux spectrum. However, the appreciably larger noise level of the SP Atlas influences our results below.

2. Data reduction.

2.1 Background normalization. — We use the magnetic-tape editions of the two atlases and discuss only their region of overlap ($\lambda\lambda$400.6-700.0 nm). Both atlases suffer from scale variations which result from the record concatenation necessary for segmented recording. This is illustrated in figure 1, where the comparison given in figure 5 of paper I is extended with the corresponding interval of the SP Atlas. The panels show the top 4 % of each atlas, and also disk-center data taken with the broad-band Fourier Transform Spectrometer at Kitt Peak (Brault, 1978, example 2), which here supply a standard of quality. Each tracing is again normalized to a straight line (dotted) connecting the peaks at λ = 401.34 nm and λ = 405.31 nm, which are the highest in the FTS data and in the JJ Atlas, respectively. The upward spikes display the background windows in this crowded region on an exaggerated scale. The differences between their envelopes in the two lower panels are due to segment-by-segment tilts of the JJ Atlas records, of which the junctions are indicated. The SP Atlas (top) shows better background normalization, at least in the left half of the figure; but its peak-to-peak variations are larger, primarily due to the larger noise.

The varying segment tilts encumber locating the *true* continua I_c^T and F_c^T, whereas the noise decreases the precision with which one can locate the *local* continuum F_c^L (see paper I for notation and definitions; we use F for irradiance and call it flux). In section 2.1 of paper I we have worked out in detail how to convert measurements normalized to the local continuum into line parameters referring to the true continuum, i.e. corrected for the presence of unresolved blends. We refrain here from applying similar corrections to measurements from the SP Atlas because the errors in the evaluation of F_c^L, which are rather large due to the noise in the background flux values, exceed the corrections, which are small. We thus provide « local » line strengths and line depths only.

2.2 Line parameters. — Of the 750 lines without resolved blends selected from the JJ Atlas in paper I, there are 638 present below the upper wavelength limit of the SP

Send offprint requests to : R. J. Rutten.

Atlas (700 nm). We have rejected 34 lines for which the adjacent maxima in the SP Atlas are so low that their halfwidths are ill-defined, and also λ588.383 and λ697.047, which should have been rejected in paper I because they are blended by telluric H_2O lines; the latter are stronger in the SP Atlas than in the JJ Atlas. For the remaining 602 lines we have measured the profile parameters listed in table I ([1]).

The first column of table I specifies the wavelength of the line in nm, measured again as the normalized first moment of the lower third of the profile, on the wavelength scale of the SP Atlas. The identification (spectrum and multiplet number) is again copied from Moore *et al.* (1966). The parameter « Mode » is W for the lines for which the whole profile was used, B if only the blue half and R if only the red half was used, as in paper I. The halving serves to reduce the effects of unresolved blends often present in one line wing; we have halved the SP Atlas profiles following the choices made in paper I for the JJ Atlas profiles.

The measurement of the other profile parameters differs from paper I in the determination of the extent of a line and of the local continuum, because the noise in the SP Atlas bars the simple definition of a line as the interval between two successive maxima. Instead, we here define a line to begin and end at the first maxima of a running mean that are outside the extent of the line as it was measured in the JJ Atlas. The running mean is given by $(F_{k-1} + 2\,F_k + F_{k+1})/4$, where k is the sample counter of the successive tape-edition irradiance values F_k. We define the local continuum F_c^L equal to the highest of these two smoothed maxima, and measure the fractional line depth $D_{SP}^L = (F_c^L - F_\lambda)/F_c^L$, the full width at half maximum in pm $FWHM_{SP}$, and the logarithmic line strength log (W_{SP}^L/λ) from this background level. The last column specifies the background, relative to the nominal continuum level of the SP Atlas F_c^{SP} (900 in tabular- and tape-edition units).

3. Discussion.

In figure 2 we show the differences between the strengths, depths and widths of the 602 lines in table I and the corresponding values given for the JJ Atlas in table IV of paper I, as functions of line strength (left) and line depth (right). Each panel shows a well-defined trend at right and large spread at left; we discuss these features separately.

What trends should we expect ? Let us first consider the effects of the solar *rotation*. Simple theory (e.g. Unsöld, 1955, pp. 508-511; Gray, 1976, pp. 393-399) shows that if the intensity profile of a line, relative to its background, does not vary over the disk, then the flux profile is simply the convolution of the intensity profile with a rotation profile of which the shape is set by the continuum limb darkening. This convolution decreases the line depths and increases the line widths, but does not affect the line strengths. The changes increase with wavelength because the solar limb is less darkened at longer wavelengths, so that the rotation profile is flatter : in the red, the west and east limbs contribute more Doppler-shifted signal than in the blue. We estimate the effect of rotational broadening from a simple numerical experiment. A plot of $FWHM_{JJ}/\lambda$ against D_{JJ}^L (not shown) shows that disk-center lines of depth $D^L = 0.5$ typically have $FWHM/\lambda = 0.015 \pm 0.002$. Smearing gaussians of this halfwidth with the solar rotation profile (with $v \sin i = 1.9$ km/s) results in lowering of their amplitudes by $10 \mp 3\,\%$ at $\lambda = 550$ nm, with less than 1 % amplitude change over the range $\lambda\lambda$400-700 nm.

In addition, there are effects of center-to-limb variations in the *intensity profiles*. Most of these lines are better described by pure absorption than by scattering; they become shallower towards the limb, which results in reduction of their depths and strengths in the flux spectrum compared with the rotationally-broadened disk-center intensity spectrum. Furthermore, the broadening effects of granulation and waves, measured traditionally as micro- and macroturbulence, increase when viewed obliquely, resulting in decrease of the line depths, increase of the line widths, and, for lines on the flat part of the curve of growth, increase of the line strengths. These profile effects also increase with wavelength due to the decrease in limb darkening, but more steeply than the rotational broadening because the whole limb contributes, rather than its east and west parts only. The largest profile effect is generally the increase of the macroturbulence from 1 km/s at disk center to 2 km/s at the limb.

Let us now compare these expectations to the actual trends in figure 2. The mean vertical offsets of the stronger lines, best seen in the D_{JJ}^L panels at right, indeed display effects of smearing : the line widths (bottom) are larger in the flux spectrum and the depths (middle) are smaller, while the strengths (top) are about the same. The reductions in line depth are somewhat larger than the prediction for rotational broadening alone, especially at longer wavelengths. They show a pronounced increase with wavelength, which we attribute to the profile effects. The long-wavelength lines in the middle panels (crosses) show upturns for the strongest lines, i.e. smaller reduction in line depth; this decrease in the effect of the smearing on their line depth results from their line-core saturation. (A similar upturn is shown by the plot of $FWHM_{JJ}/\lambda$ against D_{JJ}^L mentioned above.) The strongest blue lines present (circles) have not yet reached saturation and show no upturn.

We now turn to the *spread*. Some of it may be due to variations in the profile effects discussed above, but most of it results from measurement errors, primarily in the assignment of the local continuum F_c^L which is most sensitive to the noise in the SP Atlas. This is illustrated in the middle-right panel of figure 2, in which the increase of the spread for weak lines is most abrupt. (The fan-like structure at left is due to the three-digit discretization.) The many weak lines that quite erroneously have $D_{SP}^L > D_{JJ}^L$ testify that J_c^L has often been overestimated, notwithstanding our smoothing. The size of the spread multiplied by D^L shows that the errors in J_c^L range up to 1 %, in agreement with the general accuracy of 1 % estimated for the SP Atlas by its authors; we find that heavier smoothing in the evaluation of J_c^L does not produce significant improvement.

([1]) Copies on magnetic tape or punched cards can be obtained from E.v.d.Z.

The spread in the top panels is larger (0.1 dex = 26 %) because the equivalent widths are about twice as sensitive to errors in J_c^L as the line depths are. The many overestimations of J_c^L have caused the slight mean offsets shown by the weaker lines in the top panels.

Finally, we note that the spread in the top-left panel is two to three times smaller than the spread in the comparable bottom-left panel of figure 6 in paper I. The lines most suitable for abundance analysis, with $-5.5 \leqslant \log(W/\lambda) \leqslant -5.2$, have errors well within 0.1 dex, which is the best precision attainable using line strengths in curve-of-growth methods (see Sect. 5 of paper I).

Acknowledgements.

We thank C. Zwaan and B. J. Oranje for comments.

Note added in proof : A detailed analysis of solar rotational broadening has been given in the PhD thesis of David H. Bruning, now at Mt Wilson.

References

Beckers, J. M., Bridges, Ch. A., Gilliam, L. B. : 1976, *A High Resolution Spectral Atlas of the Solar Irradiance From 380 to 700 Nanometers,* Sacramento Peak Observatory (SP Atlas).

Brault, J. W. : 1978, in « Future Solar Optical Observations : Needs and Constraints », eds. G. Godoli, G. Noci, A. Righini, *Osser. e Memorie dell' Oss. Astrof. di Arcetri* **106,** 33.

Delbouille, L., Roland, G., Neven, L. : 1973, *Photometric Atlas of the Solar Spectrum from λ3000 to λ10000,* Institut d'Astrophysique, Liège (JJ Atlas).

Gray, D. F. : 1976, *The Observation and Analysis of Stellar Photospheres,* Wiley Sons, New York.

Moore, Ch. E., Minnaert, M. G. J., Houtgast, J. : 1966, « The Solar Spectrum 2935 Å to 8770 Å », *Nat. Bur. Stand. (U.S.) Monogr.* No. 61, Washington.

Rutten, R. J., van der Zalm, E. B. J. : 1984, *Astron. Astrophys. Suppl. Ser.* **55,** 143 (Paper I).

Unsöld, A. : 1955, *Physik der Sternatmosphären,* Springer Verlag, Berlin.

TABLE I.

Wavelength	Ident		Mode	D^L	FWHM	$\log(W^L/\lambda)$	F_L^L/F_L^{SP}
401.3233	Ti Ip	186	W	0.094	6.81	-5.739	0.993
402.1335	Nd II	36	B	0.182	5.69	-5.579	0.986
404.1907	Fe I	602	B	0.143	4.82	-5.732	0.952
404.2581	Ce II	140	B	0.152	4.81	-5.715	0.963
405.0325	Zr II	43	B	0.305	6.74	-5.255	0.990
406.0268	Ti I	80	W	0.489	6.65	-5.045	0.976
408.5723	Zr II	54	R	0.048	5.05	-6.208	0.956
409.1559	Fe I	357	W	0.672	7.93	-4.833	0.971
419.4493	Fe I	274	W	0.246	6.48	-5.394	0.979
426.5926	Mn I	23	B	0.633	8.59	-4.861	0.975
426.6218	Ti I	252	R	0.098	6.38	-5.831	0.993
428.1373	Ti I	44	B	0.333	7.27	-5.217	0.988
428.1593	Fe Ip	171	B	0.105	6.01	-5.811	0.991
431.9445	Fe I	214	B	0.205	6.71	-5.458	0.974
434.9785	Ce II	59	W	0.085	6.55	-5.852	0.970
436.4858	Cr I	153	B	0.019	7.50	-6.649	0.983
439.2308	Fe Ip	757	R	0.092	8.09	-5.687	0.981
441.0523	Ni I	88	R	0.553	9.14	-4.873	0.975
441.3403	Fe Ip	1046	B	0.086	12.49	-5.613	0.993
443.9636	Fe I	515	W	0.247	7.42	-5.347	0.994
443.9884	Fe I	116	W	0.572	8.07	-4.950	0.992
444.1273	Ti I	160	W	0.082	6.85	-5.890	0.974
444.5475	Fe I	2	R	0.508	6.82	-5.069	0.975
444.6385	Nd II	49	B	0.149	5.61	-5.698	0.982
446.5808	Ti I	146	W	0.446	8.09	-5.039	0.996
447.0485	Ni I	86	B	0.717	10.43	-4.721	0.982
448.5970	Fe Ip	825	W	0.237	7.79	-5.339	0.993
449.1655	Cr I	95	R	0.256	7.86	-5.314	0.976
449.1845	Cr I	83	W	0.127	6.81	-5.694	0.979
449.2308	Cr I	197	B	0.309	7.97	-5.210	0.994
450.4224	Fe Ip	988	B	0.030	13.76	-6.134	1.000
451.2268	Ca I	24	R	0.263	9.19	-5.219	0.996
451.2740	Ti I	42	B	0.689	9.23	-4.786	0.993
451.2995	Ni I	163	R	0.233	8.19	-5.319	0.997
451.8027	Ti I	42	R	0.688	9.22	-4.804	0.999
452.3080	Ce II	2	R	0.164	8.04	-5.468	0.980
452.3404	Fe I	829	R	0.477	8.33	-5.014	0.986
454.3223	Fe Ip	893	R	0.049	8.11	-6.059	0.988
454.6469	Fe I	1047	B	0.075	7.49	-5.898	0.983
454.8770	Ti I	42	R	0.714	9.13	-4.800	0.988
455.1650	Fe I	972	B	0.317	7.44	-5.266	0.970
455.6928	Fe I	638	R	0.300	7.72	-5.233	0.985
456.0713	V I	109	B	0.111	7.19	-5.716	0.990
456.2631	Ti I	7	R	0.147	7.12	-5.594	1.000
456.3423	Ti I	266	R	0.127	7.38	-5.656	0.981
456.6038	Fe Ip	1169	R	0.010	2.70	-7.168	1.000
456.7409	Ni I	102	W	0.043	8.55	-6.083	0.999
457.4219	Fe I	554	R	0.436	8.53	-5.047	0.976
457.5109	Cr I	196	B	0.116	7.52	-5.706	0.971
459.2055	Cr II	44	B	0.466	9.87	-4.964	0.984
459.3530	Fe I	971	W	0.315	8.69	-5.179	0.991
460.7086	Fe Ip	724	W	0.049	6.95	-6.105	0.988
462.2745	Cr I	81	B	0.223	7.81	-5.395	0.967
462.5923	Cr I	244	R	0.143	7.40	-5.610	0.984
462.9073	Zr II	139	B	0.035	6.06	-6.325	0.990
463.0785	Fe I	969	W	0.038	6.72	-6.249	0.989
463.3256	Cr I	186	W	0.110	7.55	-5.713	0.987
465.8298	Fe I	591	B	0.188	8.24	-5.460	0.972
467.0170	Fe II	25	R	0.309	8.26	-5.226	0.968
467.2837	Fe Ip	40	B	0.341	9.03	-5.146	0.966
469.0793	Ti I	76	B	0.043	5.26	-6.295	0.972
470.0611	Cr I	62	B	0.187	7.18	-5.525	0.966
470.6309	Fe Ip	890	R	0.092	6.09	-5.876	0.980
470.8016	Cr I	186	B	0.557	9.48	-4.917	0.966
470.9713	Mn I	21	R	0.629	9.95	-4.838	0.970
471.6833	Fe I	634	W	0.076	8.63	-5.793	0.980
472.0129	Fe IIp	54	B	0.048	7.88	-6.090	0.983
472.2163	Zn I	2	B	0.631	10.53	-4.771	0.989
472.6138	Fe I	384	R	0.195	7.57	-5.474	0.974
473.7353	Cr I	145	R	0.524	9.23	-4.959	0.972
474.3826	Sc I	14	B	0.080	10.81	-5.715	0.989
474.5135	Fe I	67	B	0.150	6.86	-5.650	0.966
474.8733	La II	65	B	0.051	6.78	-6.077	0.987
475.4368	Co I	156	R	0.070	6.92	-5.973	0.967
475.7850	Ru I	12	B	0.025	7.27	-6.408	0.985
475.8124	Ti I	233	B	0.471	8.45	-5.047	0.985
475.8409	Ni I	193	W	0.039	8.84	-6.094	0.988
475.9276	Ti I	233	R	0.502	8.50	-5.011	0.984
476.0068	Fe I	384	B	0.078	6.81	-5.942	0.978
476.7857	Cr I	231	B	0.194	7.87	-5.462	0.988
477.0668	Cr I	124	R	0.048	9.21	-5.980	0.983
477.3963	Ce II	17	R	0.113	8.21	-5.668	0.970
477.5140	Cr I	230	B	0.070	8.08	-5.935	0.976
477.8255	Ti I	232	B	0.167	9.00	-5.460	0.993
477.9441	Fe I	720	R	0.452	8.48	-5.059	0.995
478.0819	Fe I	633	B	0.090	9.29	-5.742	0.988
478.7493	Fe Ip	408	R	0.023	9.61	-6.395	0.979
478.8764	Fe I	588	B	0.648	9.81	-4.805	0.993
479.0563	Fe I	1068	W	0.095	6.85	-5.828	0.978
479.0758	Fe I	632	R	0.094	5.94	-5.935	0.987
479.1603	Sm II	7	R	0.041	7.35	-6.158	0.993
479.2858	Co I	158	W	0.341	9.08	-5.141	0.998
479.3428	Ni I	158	R	0.055	7.41	-6.004	0.996
479.3973	Fe I	512	B	0.099	8.43	-5.720	0.999
479.4363	Fe I	115	B	0.131	9.14	-5.535	0.998
479.4835	Ti IIp	29	B	0.029	9.70	-6.229	0.996
479.8268	Fe I	1042	R	0.446	8.45	-5.072	0.979
479.9071	Fe Ip	1098	B	0.040	7.80	-6.137	0.991
480.1028	Cr I	168	B	0.496	9.05	-4.993	0.981
480.2518	Fe I	1206	R	0.154	9.35	-5.482	0.984
480.8147	Fe I	633	W	0.306	8.04	-5.245	0.978
480.9939	Fe I	793	B	0.213	8.41	-5.389	0.987
481.3479	Co I	158	B	0.417	10.15	-5.018	0.984
482.0413	Ti I	126	R	0.427	8.69	-5.080	0.985
483.5874	Fe I	1068	B	0.497	8.96	-5.005	0.989
483.6853	Cr I	144	B	0.159	8.44	-5.524	0.986
483.7403	Ti Ip	250	B	0.028	8.20	-6.342	1.000
488.0059	Cr I	167	B	0.069	9.22	-5.840	0.972
488.5436	Fe I	966	R	0.660	9.75	-4.837	0.981
489.2863	Fe I	1070	B	0.514	9.32	-4.960	0.976
490.5138	Fe I	986	B	0.323	8.47	-5.195	0.976
490.8608	Fe I	115	R	0.080	8.50	-5.786	0.983
491.3976	Ni I	132	R	0.534	9.39	-4.926	0.981
491.5236	Ti I	157	W	0.086	7.17	-5.849	0.986
491.7234	Fe I	1066	B	0.577	9.80	-4.903	0.979
492.6153	Ti I	39	R	0.079	8.69	-5.814	0.999
493.5839	Ni I	177	R	0.565	9.72	-4.899	0.988
493.6341	Cr I	166	B	0.446	8.98	-5.062	0.980
495.3214	Ni I	111	R	0.534	9.39	-4.930	0.998
495.3719	Cr I	166	R	0.058	7.99	-5.975	0.997
495.4293	Fe Ip	1093	B	0.017	3.33	-6.850	0.986
496.1919	Fe I	845	B	0.270	8.70	-5.294	0.986
496.2577	Fe I	1097	R	0.520	9.62	-4.935	0.986
496.4719	Ti I	173	B	0.094	8.02	-5.793	0.988
496.4931	Cr I	9	B	0.423	8.22	-5.130	0.974
496.6813	Cr I	259	R	0.027	8.28	-6.340	0.986
496.7528	Ni I	141	R	0.148	8.84	-5.550	0.972
497.6698	Ni Ip	254	W	0.073	7.84	-5.895	0.984
498.7623	Fe Ip	1094	W	0.037	7.73	-6.222	0.983
499.2789	Fe I	1110	B	0.101	8.97	-5.708	0.983
499.3353	Fe II	36	B	0.378	9.23	-5.110	0.988
499.5411	Fe I	1113	R	0.151	8.53	-5.570	0.976
499.5655	Ni I	145	B	0.200	7.95	-5.482	0.975
500.3748	Ni I	50	B	0.370	8.35	-5.176	0.978
500.4898	Mn I	20	B	0.151	8.99	-5.509	0.987
501.0943	Ni I	144	R	0.487	9.13	-5.008	0.987
501.6481	Fe I	1089	B	0.337	8.90	-5.180	0.989
502.2874	Ti I	38	B	0.675	10.30	-4.820	0.979
502.6488	Ni I	158	B	0.031	7.08	-6.338	0.983
504.7118	Fe Ip	1242	R	0.044	8.00	-6.165	0.973
504.8854	Ni I	195	R	0.556	10.04	-4.898	0.968
505.8503	Fe I	884	B	0.135	8.01	-5.660	0.994
506.2103	Ti I	199	B	0.156	8.84	-5.544	0.991
506.4068	Ti I	294	B	0.065	9.20	-5.893	0.996
507.1488	Ti I	110	B	0.267	10.57	-5.228	0.977
509.4414	Ni I	164	R	0.317	9.28	-5.207	0.993
511.2488	Cr I	19	B	0.046	6.73	-6.210	0.992
511.3444	Ti I	109	B	0.284	8.33	-5.310	0.982
511.9893	Fe Ip	960	R	0.051	9.31	-6.014	0.989
512.2113	Cr I	19	B	0.127	7.45	-5.714	0.977
514.1751	Fe I	114	B	0.711	12.29	-4.701	0.999
514.5468	Ti I	109	B	0.373	9.00	-5.140	0.977
514.5739	Fe Ip	931	R	0.059	9.91	-5.780	0.992
515.2188	Ti I	4	R	0.389	8.50	-5.162	0.986
515.7985	Ni I	111	B	0.202	8.55	-5.448	0.989
515.9958	Fe Ip	1095	R	0.049	7.71	-6.127	0.993
518.7918	Fe I	1032	R	0.494	9.40	-4.972	0.980
519.6063	Fe I	1091	R	0.615	10.53	-4.850	0.974
519.7165	Ni I	204	B	0.256	10.30	-5.251	0.988
520.0173	Cr I	201	B	0.219	10.77	-5.295	0.990
520.6806	Fe Ip	1095	R	0.071	9.49	-5.812	0.988
521.3808	Fe I	962	B	0.076	8.98	-5.862	0.990
521.4133	Cr I	193	B	0.182	8.54	-5.494	0.988
521.9705	Ti I	4	R	0.279	8.51	-5.285	0.990
522.3188	Fe I	880	B	0.300	9.11	-5.243	0.985
523.0983	Ti I	215	W	0.020	8.54	-6.471	0.983
523.4631	Fe II	49	W	0.649	11.66	-4.790	0.981
523.7325	Cr II	43	W	0.446	10.82	-4.999	0.982
523.8256	Fe I	962	W	0.032	10.32	-6.141	0.991
523.8963	Cr I	59	B	0.176	8.64	-5.485	0.990
524.0873	V I	131	W	0.050	10.92	-5.931	0.988
524.1463	Cr I	59	W	0.043	8.86	-6.081	0.990
524.3783	Fe I	1089	R	0.543	10.17	-4.936	0.980
524.7289	Ti I	183	B	0.087	6.72	-5.932	0.975
525.0218	Fe I	1	R	0.647	9.12	-4.910	0.971
525.3029	Fe Ip	113	B	0.205	8.88	-5.414	0.994
525.4643	Co I	187	B	0.045	6.78	-6.161	0.976
525.5516	Nd II	43	B	0.066	6.48	-6.077	0.966
525.9739	Pr II	35	B	0.033	8.86	-6.209	0.994
525.9973	Ti I	298	W	0.064	9.11	-5.931	0.989
526.2623	Fe Ip	1149	R	0.101	10.07	-5.681	0.984
526.4807	Fe II	48	W	0.417	10.01	-5.060	0.989
527.9668	Fe Ip	584	B	0.047	11.84	-5.937	0.993
528.0626	Co I	172	R	0.162	11.61	-5.416	0.983
528.2403	Ti I	74	R	0.184	11.08	-5.360	0.976
528.7180	Cr I	225	R	0.116	8.98	-5.619	0.996
528.9835	Y II	20	B	0.042	11.85	-6.039	0.985
529.3383	Cr I	192	B	0.046	9.63	-6.079	0.990
529.4553	Fe I	875	B	0.149	9.55	-5.539	0.991
529.5318	Fe I	1146	W	0.291	9.33	-5.242	0.994
529.5783	Ti I	74	R	0.131	8.95	-5.602	0.999
529.9980	Ti I	74	W	0.155	12.42	-5.389	0.988
530.0413	Fe I	1240	B	0.049	10.33	-5.990	0.986
530.0750	Cr I	18	B	0.544	9.91	-4.963	0.981
530.1333	Fe Ip	1162	B	0.029	11.25	-6.180	0.984
530.3223	V II	54	B	0.038	9.36	-6.155	0.988
530.4183	Cr I	225	R	0.148	9.58	-5.543	0.991
530.5866	Cr II	24	B	0.234	9.76	-5.322	0.990
530.8428	Cr II	43	B	0.230	10.38	-5.315	0.993
530.8683	Fe I	1091	B	0.060	8.34	-6.024	0.979

TABLE I *(continued)*.

Wavelength	Ident		Mode	D^L	FWHM	$\log(W/\lambda)^L$	F_c^L/F_c^{SP}
531.0693	Cr II	43	R	0.120	9.89	-5.608	0.989
531.1638	Hf II	37	R	0.027	6.96	-6.503	0.979
531.2653	Co I	197	B	0.062	8.81	-5.958	0.983
531.2858	Cr I	225	R	0.183	9.93	-5.429	0.983
531.8353	Sc II	22	B	0.116	9.58	-5.634	0.988
531.8768	Cr I	225	W	0.153	9.12	-5.544	0.985
532.0040	Fe I	877	B	0.191	9.22	-5.460	0.979
532.1111	Fe I	1165	R	0.382	10.04	-5.065	0.991
532.5283	Co I	192	W	0.084	9.43	-5.795	0.976
532.5557	Fe II	49	R	0.383	10.29	-5.084	0.981
532.6819	Fe I	1147	B	0.126	9.93	-5.617	0.978
534.2707	Co I	190	B	0.293	9.95	-5.199	0.992
534.4763	Cr I	225	R	0.085	9.05	-5.785	0.993
534.7719	Ni I	145	B	0.049	9.65	-6.033	0.990
534.8323	Cr I	18	R	0.737	12.48	-4.710	0.996
535.2048	Co I	172	W	0.198	10.67	-5.381	0.991
535.6093	Sc I	17	R	0.020	12.23	-6.409	1.000
535.7186	Sc II	30	B	0.048	8.51	-6.087	0.988
535.8123	Fe Ip	628	R	0.102	8.16	-5.720	0.988
535.9203	Co I	194	W	0.099	9.33	-5.713	0.990
537.6834	Fe I	1132	B	0.154	8.76	-5.589	0.986
537.7043	La II	95	B	0.038	5.87	-6.336	0.986
537.9579	Fe I	928	R	0.543	10.38	-4.919	0.992
538.0323	C I	11	B	0.129	14.19	-5.438	0.985
538.6336	Fe I	1064	B	0.311	9.70	-5.212	0.988
538.9487	Fe I	1145	R	0.631	11.41	-4.822	0.973
539.2333	Ni I	250	B	0.119	9.32	-5.659	0.983
539.5219	Fe I	1143	B	0.198	9.20	-5.432	0.988
539.8288	Fe I	1145	R	0.586	10.92	-4.877	0.988
540.1269	Fe I	1146	B	0.244	9.45	-5.325	0.992
540.2782	Y II	35	B	0.122	9.31	-5.656	0.986
540.6778	Fe I	1148	R	0.343	9.88	-5.132	0.996
541.2790	Fe Ip	1162	R	0.182	9.26	-5.475	0.982
541.7041	Fe I	1148	B	0.319	9.74	-5.160	0.993
542.2157	Fe Ip	1145	R	0.100	8.64	-5.773	0.980
542.5252	Fe II	49	R	0.367	10.36	-5.097	0.986
542.6256	Ti I	3	B	0.068	9.01	-5.910	0.984
543.6299	Fe I	1161	B	0.366	10.17	-5.116	0.989
543.8043	Fe I	1237	B	0.026	9.59	-6.322	0.988
543.8309	Ti I	108	W	0.036	9.61	-6.150	0.981
544.3403	Fe Ip	1059	B	0.039	10.61	-6.091	0.995
544.8913	Ti I	259	R	0.016	7.11	-6.703	0.988
546.4289	Fe I	1030	R	0.355	9.88	-5.141	0.990
546.8106	Ni I	192	B	0.126	8.78	-5.629	0.991
547.0093	Fe I	1144	B	0.235	10.30	-5.312	0.988
547.1199	Ti I	106	B	0.085	10.19	-5.745	0.996
547.3383	Y II	27	B	0.056	8.85	-6.076	0.972
547.4225	Ti I	108	R	0.107	9.58	-5.712	0.983
547.4459	Ti I	259	R	0.036	6.88	-6.301	0.986
548.4633	Sc I	16	B	0.030	11.61	-6.218	0.993
549.0153	Ti I	107	B	0.217	9.01	-5.423	0.981
549.1836	Fe I	1031	R	0.123	9.81	-5.634	0.990
549.4468	Fe I	1024	B	0.248	9.86	-5.308	0.978
550.3893	Ti I	287	B	0.133	7.88	-5.692	0.976
552.0498	Sc I	15	B	0.072	9.50	-5.881	0.990
552.1298	Fe Ip	1162	B	0.049	8.27	-6.110	0.972
552.2449	Fe I	1108	W	0.394	9.88	-5.112	0.984
552.4245	Fe I	1059	R	0.042	9.85	-6.110	0.988
552.6815	Sc II	31	B	0.616	11.80	-4.837	0.986
553.7113	Ni I	188	B	0.031	10.25	-6.256	0.994
553.9281	Fe I	871	W	0.167	9.43	-5.495	0.983
554.6993	Fe I	1061	B	0.223	9.61	-5.367	0.977
555.2238	Sc II	25	R	0.044	7.34	-6.175	0.982
555.2698	Fe Ip	1281	B	0.072	10.39	-5.857	0.983
556.0218	Fe I	1164	B	0.456	10.54	-5.020	0.992
556.8870	Fe I	869	B	0.096	9.70	-5.789	0.982
557.7026	Fe I	1314	R	0.110	10.36	-5.652	0.993
557.8725	Ni I	47	R	0.484	10.34	-5.000	0.985
558.7578	Fe I	1026	B	0.325	10.03	-5.204	0.970
558.7863	Ni I	70	R	0.499	10.22	-5.000	0.976
558.9363	Ni I	205	R	0.260	9.70	-5.289	0.994
559.3741	Ni I	206	B	0.371	11.05	-5.070	0.989
559.5063	Fe Ip	1314	W	0.059	9.55	-5.970	0.983
560.6993	Ni I	205	B	0.031	6.27	-6.416	0.990
560.8980	Fe Ip	1108	W	0.099	10.20	-5.665	0.995
560.9966	Fe Ip	866	R	0.049	11.54	-6.004	0.992
561.1356	Fe Ip	869	B	0.091	8.55	-5.823	0.982
561.8639	Fe I	1107	W	0.440	10.54	-5.044	0.984
561.9603	Fe I	1161	W	0.298	10.38	-5.211	0.986
562.2213	Si I	11	R	0.044	12.69	-5.955	0.990
562.8643	Cr I	203	W	0.136	9.87	-5.585	0.990
563.5825	Fe I	1088	B	0.317	10.18	-5.199	0.989
563.6698	Fe I	868	B	0.194	8.88	-5.485	0.991
563.8755	Ni I	203	R	0.088	9.00	-5.824	0.987
564.1439	Fe I	1087	R	0.499	12.87	-4.915	0.978
564.2369	Cr I	239	B	0.051	10.08	-6.011	0.984
564.3083	Ni I	259	W	0.139	10.39	-5.560	0.986
564.6123	V I	37	R	0.038	9.31	-6.175	0.991
564.7233	Co I	112	W	0.127	10.82	-5.564	0.989
564.8268	Cr I	239	W	0.041	10.39	-6.091	0.988
564.8573	Ti I	269	W	0.099	9.57	-5.748	0.987
564.9373	Cr I	239	B	0.063	9.13	-5.955	0.989
564.9988	Fe I	1314	R	0.312	10.59	-5.182	0.989
565.1475	Fe Ip	1161	B	0.178	10.65	-5.453	0.995
565.2318	Fe I	1108	B	0.239	9.57	-5.348	0.991
565.7453	V I	37	W	0.051	10.37	-5.989	0.992
566.1023	Fe Ip	1234	R	0.040	9.61	-6.116	0.988
566.1343	Fe I	1108	R	0.205	11.00	-5.343	0.990
566.2153	Ti I	249	B	0.192	8.97	-5.503	0.966
566.5558	Si I	10	R	0.298	12.76	-5.119	0.988
567.0853	V I	36	R	0.150	12.16	-5.460	0.985
567.7698	Fe Ip	1057	B	0.060	11.15	-5.917	0.984
567.8383	Fe Ip	982	R	0.043	10.44	-6.073	0.986
567.9929	Ti I	269	B	0.044	9.73	-6.126	0.982
568.0246	Fe I	1026	R	0.102	10.12	-5.699	0.990
568.6836	Sc I	12	R	0.075	9.86	-5.869	0.979
569.0429	Si I	10	B	0.388	12.40	-5.018	0.985
570.1105	Si I	10	B	0.295	12.17	-5.166	0.987
570.1553	Fe I	209	R	0.639	11.90	-4.834	0.983
570.2323	Cr I	203	W	0.203	12.12	-5.331	0.994
570.2663	Ti I	249	B	0.070	10.58	-5.849	0.993
571.3898	Ti I	249	W	0.038	8.70	-6.198	0.992
571.7838	Fe I	1107	B	0.490	11.59	-4.936	0.978
571.9813	Cr I	119	B	0.044	7.09	-6.182	0.988
572.5658	V I	135	W	0.018	11.45	-6.470	0.989
572.7653	V I	35	B	0.063	11.50	-5.886	0.990
572.9203	Cr I	257	W	0.028	12.83	-6.228	0.996
573.1770	Fe I	1087	R	0.479	10.99	-4.971	0.993
573.7069	V I	35	B	0.081	12.86	-5.745	0.985
573.8238	Fe I	1084	B	0.115	10.99	-5.634	0.989
573.9473	Ti I	228	B	0.078	9.20	-5.868	0.991
574.1853	Fe I	1086	W	0.280	10.38	-5.257	0.984
574.2968	Fe I	1084	B	0.102	9.41	-5.755	0.982
574.8359	Ni I	45	R	0.266	9.90	-5.281	0.994
575.2037	Fe I	1180	R	0.448	11.04	-5.020	0.990
575.4408	Fe I	866	W	0.102	8.54	-5.817	0.961
575.9259	Fe I	1184	B	0.070	8.48	-5.959	0.983
576.0346	Fe I	867	B	0.213	9.39	-5.422	0.988
576.0835	Ni I	231	W	0.295	10.54	-5.227	0.976
576.6338	Ti I	309	R	0.081	9.21	-5.831	0.992
577.5081	Fe I	1087	R	0.478	11.27	-4.976	0.999
577.8458	Fe I	209	W	0.208	9.86	-5.407	0.994
578.3065	Cr I	188	R	0.276	11.13	-5.231	0.986
578.4659	Fe I	686	B	0.237	9.95	-5.353	0.984
578.5973	Ti I	309	W	0.099	10.58	-5.717	0.976
579.3073	Si I	9	B	0.306	12.77	-5.139	0.982
579.3916	Fe I	1086	R	0.295	10.54	-5.221	0.988
580.5223	Ni I	234	W	0.332	11.70	-5.132	0.989
580.6729	Fe I	1180	R	0.419	11.39	-5.040	0.985
580.9883	Fe Ip	1084	B	0.021	12.63	-6.370	0.990
581.1915	Fe I	1022	B	0.103	9.50	-5.745	0.990
581.2833	Ti I	309	B	0.021	11.19	-6.406	0.990
581.4808	Fe I	1086	W	0.199	10.87	-5.385	0.993
581.9933	V II	99	B	0.030	13.58	-6.157	0.991
582.3178	Fe II	164	W	0.018	9.87	-6.496	0.988
582.4413	Fe IIp	58	B	0.026	10.63	-6.320	0.991
582.7878	Fe Ip	552	R	0.105	10.46	-5.673	0.994
583.2483	Ti I	309	W	0.019	11.26	-6.404	0.993
583.5103	Fe Ip	1084	B	0.123	9.64	-5.661	0.983
583.7708	Fe I	1129	B	0.087	10.54	-5.769	0.989
583.8673	Cr I	119	R	0.038	9.93	-6.174	0.988
584.4593	Cr I	119	B	0.040	7.39	-6.264	0.986
584.4916	Fe I	1056	B	0.031	8.09	-6.318	0.990
584.7000	Ni I	44	B	0.204	10.05	-5.421	0.993
584.9693	Fe Ip	922	W	0.075	9.76	-5.869	0.992
585.2223	Fe I	1178	W	0.343	10.89	-5.131	0.995
585.3153	Fe I	35	B	0.069	9.66	-5.914	0.991
585.5083	Fe I	1179	B	0.194	10.94	-5.411	0.993
585.6093	Fe I	1128	R	0.295	10.52	-5.226	0.992
585.8788	Fe Ip	1084	R	0.118	9.96	-5.649	0.991
585.9597	Fe I	1181	R	0.544	12.11	-4.898	0.984
586.1113	Fe Ip	1084	R	0.076	10.11	-5.832	0.989
586.2363	Fe I	1180	W	0.592	13.08	-4.815	0.985
586.6457	Ti I	72	R	0.410	10.79	-5.076	0.993
586.7568	Ca I	46	B	0.211	11.97	-5.317	0.993
587.6288	Fe Ip	1084	W	0.032	8.88	-6.316	0.975
587.9498	Fe Ip	1201	B	0.091	10.86	-5.709	0.990
588.0033	Fe I	1201	W	0.105	10.44	-5.702	0.988
588.0289	Ti I	71	B	0.052	11.66	-6.002	0.986
588.1285	Fe Ip	1178	R	0.129	10.05	-5.596	0.986
588.4448	Cr I	119	B	0.023	8.91	-6.450	0.983
590.2466	Fe I	1234	B	0.129	8.02	-5.723	0.993
590.3313	Ti I	71	B	0.050	10.58	-6.034	0.999
590.5675	Fe I	1181	R	0.455	11.67	-4.982	0.994
590.6508	Ti I	105	B	0.043	10.79	-6.079	0.988
592.2118	Ti I	72	W	0.181	10.41	-5.467	0.998
592.7794	Fe I	1175	B	0.353	11.34	-5.124	0.992
592.9683	Fe I	1176	B	0.329	11.24	-5.175	0.985
593.0189	Fe I	1180	W	0.588	13.55	-4.814	0.985
593.3803	Fe Ip	1198	B	0.049	11.86	-5.977	0.985
593.4664	Fe I	982	W	0.543	12.93	-4.862	0.992
594.7508	Fe I	1199	B	0.074	11.63	-5.821	0.986
594.8548	Si I	16	R	0.511	14.00	-4.827	0.972
595.6698	Fe I	14	B	0.462	10.38	-5.060	0.989
596.9563	Fe I	1086	R	0.037	11.65	-6.112	0.990
597.6783	Fe I	959	W	0.492	12.35	-4.957	0.961
597.8548	Ti I	154	W	0.208	10.27	-5.419	0.977
598.2888	Cr I	185	B	0.032	14.00	-6.134	0.986
598.4825	Fe I	1260	B	0.552	13.92	-4.820	0.975
599.1378	Fe II	46	R	0.248	10.69	-5.314	0.982
599.6738	Ni I	249	W	0.165	11.05	-5.485	0.980
600.0683	Co I	169	R	0.031	8.88	-6.280	0.989
600.3019	Fe I	959	W	0.566	13.32	-4.846	0.983
600.7967	Fe I	1178	R	0.458	11.71	-4.995	0.978
600.8565	Fe I	982	R	0.582	13.36	-4.825	0.981
601.5249	Fe Ip	63	W	0.046	9.41	-6.127	0.987
601.6643	Mn I	27	B	0.569	16.07	-4.782	0.984
601.9373	Fe Ip	780	B	0.046	12.79	-5.989	0.991
602.5768	Ni I	251	W	0.042	11.32	-6.066	0.997
602.7058	Fe I	1018	B	0.501	11.98	-4.974	0.989

TABLE I *(continued)*.

Wavelength	Ident	Mode	D^L	FWHM	$\log(W/\lambda)^L$	F_c^L/F_c^{SP}
603.4033	Fe Ip 1142	W	0.072	10.16	-5.895	0.992
603.9729	V I 34	W	0.115	9.89	-5.689	0.988
605.3683	Ni I 247	R	0.159	11.31	-5.484	0.989
605.4079	Fe I 1142	B	0.079	11.72	-5.797	0.990
605.6011	Fe I 1259	B	0.515	13.47	-4.890	0.990
606.4633	Ti I 69	B	0.072	9.93	-5.878	0.988
606.5495	Fe I 207	B	0.696	15.98	-4.700	0.978
606.7638	Si I 15	R	0.024	9.23	-6.419	0.992
607.8496	Fe I 1259	R	0.518	13.25	-4.894	0.984
607.9015	Fe I 1176	R	0.363	11.50	-5.113	0.988
608.1449	V I 34	B	0.117	10.71	-5.660	0.986
608.4103	Fe II 46	B	0.168	9.95	-5.524	0.990
608.6288	Ni I 249	B	0.332	11.73	-5.141	0.991
608.6683	Co I 165	B	0.022	13.45	-6.294	0.990
608.9570	Fe I 1327	B	0.296	11.61	-5.193	0.992
609.0216	V I 34	R	0.280	10.83	-5.262	0.991
609.1173	Ti I 238	B	0.129	9.77	-5.654	0.991
609.3153	Co I 37	B	0.067	13.66	-5.808	0.989
609.3646	Fe I 1177	B	0.252	11.19	-5.307	0.990
609.4376	Fe I 1177	R	0.161	11.11	-5.479	0.991
609.6668	Fe I 959	R	0.302	11.41	-5.214	0.988
609.8249	Fe Ip 1200	B	0.136	10.52	-5.609	0.988
609.8669	Ti I 304	B	0.045	11.88	-6.063	0.986
611.1075	Ni I 230	B	0.275	11.88	-5.221	0.996
611.1663	V I 34	W	0.083	13.36	-5.701	0.994
611.8109	Ni I 230	B	0.024	14.37	-6.332	0.991
612.0253	Fe I 14	B	0.049	9.37	-6.077	0.988
612.1013	Ti I 153	R	0.031	8.78	-6.340	0.984
612.5023	Si I 30	W	0.207	13.59	-5.282	0.988
612.6223	Ti I 69	R	0.195	10.18	-5.441	0.990
612.8981	Ni I 42	W	0.231	10.12	-5.379	0.989
613.0138	Ni I 248	B	0.184	10.48	-5.465	0.990
613.3963	Ni I 229	W	0.044	11.22	-6.075	0.986
613.5368	V I 34	B	0.080	11.25	-5.812	0.979
614.5016	Si I 29	R	0.256	13.95	-5.179	0.989
614.9248	Fe II 74	R	0.282	11.94	-5.229	0.987
615.1623	Fe I 62	W	0.420	11.06	-5.083	0.989
615.5703	Si I 29	R	0.047	11.41	-6.024	0.982
615.6803	O I 10	R	0.034	11.97	-6.135	0.990
615.7731	Fe I 1015	B	0.471	11.83	-5.008	0.980
615.9383	Fe I 1175	B	0.101	12.42	-5.667	0.987
616.0748	Na I 5	B	0.383	13.38	-5.044	0.983
616.5363	Fe I 1018	R	0.365	11.52	-5.120	0.985
616.6440	Ca I 20	R	0.504	12.67	-4.935	0.985
617.3343	Fe I 62	R	0.527	12.20	-4.922	0.986
617.6818	Ni I 228	W	0.452	13.03	-4.967	0.988
617.7245	Ni I 58	W	0.128	9.87	-5.647	0.983
618.6713	Ni I 229	R	0.236	11.42	-5.328	0.989
618.7408	Fe Ip 342	B	0.028	10.53	-6.334	0.984
618.7993	Fe I 959	R	0.368	12.11	-5.092	0.991
619.9506	Fe I 208	R	0.042	9.88	-6.106	0.992
620.0321	Fe I 207	B	0.542	12.61	-4.921	0.986
620.4613	Ni I 226	B	0.176	11.83	-5.448	0.989
621.3438	Fe I 62	W	0.595	12.79	-4.871	0.992
621.3873	V I 20	B	0.043	10.30	-6.084	0.993
621.6358	V I 19	W	0.262	12.93	-5.215	0.993
622.0479	Ti I 293	R	0.075	9.83	-5.895	0.984
622.0783	Fe I 958	B	0.151	10.31	-5.580	0.983
622.3989	Ni I 228	B	0.222	11.44	-5.360	0.992
622.4513	V I 20	B	0.051	10.19	-6.060	0.992
622.6739	Fe I 981	R	0.237	11.70	-5.301	1.000
623.0093	Ni I 227	B	0.157	10.53	-5.538	0.982
623.2649	Fe I 816	W	0.557	13.60	-4.856	0.990
623.3193	V I 20	R	0.038	12.91	-6.071	0.995
623.9353	Sc I 2	B	0.053	9.04	-6.117	0.987
623.9943	Fe II 74	R	0.090	10.89	-5.802	0.979
624.0651	Fe I 64	R	0.409	11.31	-5.087	0.993
624.2839	V I 19	B	0.073	13.50	-5.803	0.988
624.3113	V I 19	B	0.218	11.69	-5.372	0.983
624.5618	Sc II 28	B	0.265	11.69	-5.276	0.987
625.1833	V I 19	W	0.116	12.72	-5.579	0.998
625.2573	Fe I 169	R	0.687	15.37	-4.711	0.992
625.8111	Ti I 104	W	0.412	11.40	-5.091	0.991
626.5143	Fe I 62	W	0.599	13.22	-4.847	0.997
627.0233	Fe I 342	R	0.429	11.27	-5.057	0.999
627.4663	V I 19	W	0.070	11.18	-5.809	0.996
628.5168	V I 19	W	0.087	10.90	-5.790	1.000
629.0553	Fe Ip 208	B	0.040	12.43	-6.096	0.995
630.0688	Sc II 28	B	0.052	12.06	-5.974	0.992
630.3463	Fe I 1140	W	0.040	11.37	-6.109	0.990
630.3763	Ti I 104	W	0.070	11.29	-5.862	0.994
631.1505	Fe I 342	R	0.230	11.58	-5.330	0.993
631.5818	Fe I 1014	B	0.330	11.89	-5.176	0.991
631.6583	Ni I 248	B	0.029	10.31	-6.312	0.988
632.0423	La II 19	R	0.036	12.03	-6.126	0.993
632.0849	Sc II 28	B	0.068	12.74	-5.849	0.995
632.2173	Ni I 249	R	0.137	11.98	-5.507	0.993
632.2693	Fe I 207	W	0.542	12.99	-4.904	0.995
632.6853	V I 84	B	0.020	10.53	-6.441	0.998
632.7605	Ni I 44	W	0.314	11.58	-5.196	0.999
633.0098	Cr I 6	R	0.236	11.34	-5.310	1.000
633.0858	Fe I 1254	B	0.260	12.09	-5.282	0.986
633.5338	Fe I 62	B	0.634	13.89	-4.810	0.989
633.6099	Ti I 103	B	0.052	8.66	-6.098	0.989
635.3843	Fe Ip 13	B	0.013	9.84	-6.803	0.989
636.9466	Fe II 40	R	0.144	10.83	-5.580	1.000
637.6193	Fe Ip 1140	B	0.018	5.44	-6.668	0.994
637.8255	Ni I 247	B	0.248	12.91	-5.274	0.997
638.0749	Fe I 1015	B	0.397	11.78	-5.099	0.993
638.5713	Fe Ip 1253	R	0.085	12.89	-5.746	1.000
639.2543	Fe I 109	B	0.156	11.16	-5.545	0.994
639.3613	Fe I 168	R	0.692	16.75	-4.690	0.983
641.6923	Fe II 74	B	0.300	11.83	-5.207	0.992
642.9913	Co I 81	B	0.026	15.28	-6.209	0.997
643.2685	Fe II 40	B	0.302	12.28	-5.211	0.992
643.6413	Fe I 1016	B	0.082	11.34	-5.806	0.991
644.0933	Mn I 39	W	0.048	12.54	-5.987	0.997
645.2330	V I 48	R	0.057	10.62	-5.942	1.000
645.5008	Co I 174	B	0.085	15.66	-5.670	0.989
645.6390	Fe II 74	B	0.435	13.42	-5.003	0.992
646.4673	Ca I 19	B	0.100	10.38	-5.779	0.991
647.1673	Ca I 18	R	0.604	13.81	-4.843	0.989
647.7853	Co I 174	R	0.030	11.16	-6.276	0.995
648.1875	Fe I 109	W	0.476	12.18	-5.012	0.987
648.2806	Ni I 66	W	0.317	12.32	-5.173	0.994
649.8942	Fe I 13	W	0.378	10.73	-5.170	0.988
649.9653	Ca I 18	R	0.577	13.56	-4.870	0.994
650.8853	Ca I 18	R	0.079	10.77	-5.802	0.994
651.6089	Fe II 40	R	0.386	12.84	-5.077	0.991
651.8376	Fe I 342	B	0.435	11.86	-5.065	0.978
653.1423	V I 48	B	0.049	11.42	-6.058	1.000
653.2879	Ni I 64	B	0.131	11.33	-5.623	0.998
653.3936	Fe I 1197	B	0.292	12.57	-5.217	0.996
658.6319	Ni I 64	B	0.312	12.84	-5.180	0.990
659.1329	Fe I 1229	B	0.079	13.79	-5.765	0.994
659.3880	Fe I 168	R	0.551	13.93	-4.891	0.986
659.8602	Ni I 249	R	0.188	13.54	-5.346	0.999
659.9116	Ti I 49	B	0.077	10.97	-5.889	0.992
660.4596	Sc II 19	R	0.268	12.62	-5.234	0.998
660.6963	Ti IIp 91	B	0.054	11.88	-6.008	0.983
660.8033	Fe I 109	W	0.147	11.39	-5.546	0.997
662.5023	Fe I 13	R	0.127	12.13	-5.596	0.995
662.7549	Fe I 1174	B	0.207	12.28	-5.378	0.991
663.0013	Cr I 16	R	0.052	12.66	-5.932	0.995
663.2443	Co I 111	R	0.057	12.85	-5.911	0.987
663.3753	Fe I 1197	W	0.428	13.23	-5.036	0.965
663.5128	Ni I 264	R	0.177	12.41	-5.451	0.985
666.1083	Cr I 282	B	0.087	13.44	-5.730	0.993
666.1338	Ni I 246	R	0.051	10.75	-6.063	0.994
666.7433	Fe I 168	B	0.045	13.25	-6.026	0.992
666.7716	Fe I 1228	B	0.066	9.19	-6.008	0.988
668.7493	Y I 1	W	0.032	11.81	-6.210	1.000
669.8678	Al I 5	W	0.141	13.81	-5.488	0.994
669.9143	Fe I 1228	B	0.061	10.52	-6.003	0.993
670.3575	Fe I 268	R	0.286	12.08	-5.256	0.994
670.4493	Fe I 1052	B	0.050	13.27	-5.957	0.999
671.0323	Fe I 34	W	0.123	11.49	-5.651	0.992
671.3743	Fe I 1255	R	0.159	12.25	-5.498	0.996
672.5356	Fe I 1052	B	0.131	10.76	-5.626	0.991
672.6673	Fe I 1197	B	0.329	13.07	-5.157	0.991
673.3158	Fe I 1195	R	0.195	12.19	-5.408	0.999
673.6513	Fe Ip 1122	B	0.015	8.44	-6.749	0.998
673.9523	Fe I 34	R	0.095	11.16	-5.756	0.996
674.3128	Ti I 48	R	0.137	12.81	-5.561	0.991
674.5968	Fe I 1005	B	0.051	13.33	-5.960	0.992
675.0158	Fe I 111	W	0.514	13.47	-4.954	0.993
675.3463	Fe Ip 1196	W	0.050	12.02	-6.009	0.996
675.6543	Fe Ip 1120	W	0.026	15.82	-6.242	0.996
676.7785	Ni I 57	R	0.542	13.16	-4.927	0.991
677.2323	Ni I 127	R	0.353	12.57	-5.136	0.992
678.6863	Fe I 1052	W	0.188	12.28	-5.426	0.995
679.3263	Fe I 1005	B	0.100	11.45	-5.741	0.996
679.6128	Fe I 1007	W	0.078	13.16	-5.792	0.989
679.8456	Ca I 31	B	0.038	11.00	-6.230	0.985
680.1852	Fe Ip 34	W	0.016	9.40	-6.693	0.997
680.4278	Fe I 1225	R	0.111	11.23	-5.689	0.992
680.6850	Fe I 268	B	0.276	10.81	-5.326	0.999
681.0266	Fe I 1197	B	0.349	13.31	-5.125	0.991
681.4958	Co I 54	R	0.119	12.11	-5.598	0.996
682.0375	Fe I 1197	B	0.281	13.43	-5.213	0.987
682.4843	Fe Ip 1280	B	0.022	10.91	-6.467	0.994
683.3238	Fe I 1194	B	0.072	11.76	-5.862	0.991
683.7008	Fe I 1225	R	0.135	11.94	-5.584	0.991
683.9843	Fe I 205	R	0.234	11.08	-5.373	0.988
684.2048	Ni I 126	R	0.196	12.07	-5.417	0.989
684.3663	Fe I 1173	B	0.413	13.66	-5.041	0.991
684.8573	Si I 37	B	0.103	16.77	-5.540	0.998
685.0443	Ni I 157	B	0.057	17.63	-5.796	0.998
685.1632	Fe I 34	R	0.035	13.14	-6.193	0.999
685.5723	Fe I 1194	B	0.130	12.62	-5.579	0.992
685.7253	Fe I 1006	W	0.171	12.05	-5.480	0.998
685.8153	Fe I 1173	R	0.359	13.52	-5.100	0.999
686.1248	Ni I 293	W	0.025	10.50	-6.379	0.991
686.1943	Fe I 109	R	0.147	11.98	-5.540	0.999
686.2496	Fe I 1191	W	0.222	12.51	-5.349	0.998
686.4318	Fe Ip 1186	B	0.052	12.55	-5.933	0.997
688.0633	Fe I 1051	B	0.100	11.88	-5.735	0.988
688.2518	Cr I 222	B	0.221	13.19	-5.346	0.989
688.3059	Cr I 222	B	0.211	13.04	-5.368	0.989
689.8299	Fe I 1078	W	0.119	12.39	-5.630	0.980
691.6689	Fe I 1052	B	0.364	13.29	-5.135	0.959
692.5283	Cr I 222	B	0.255	13.82	-5.221	0.988
692.6103	Cr I 222	B	0.132	13.20	-5.554	0.988
693.6509	Fe I 1196	B	0.052	12.71	-5.997	0.994
695.1253	Fe I 1186	W	0.407	12.26	-5.089	0.983
696.0333	Fe I 1222	R	0.088	11.58	-5.819	0.982
697.1953	Fe I 404	R	0.098	10.55	-5.798	0.991
697.8860	Fe I 111	W	0.513	14.15	-4.955	0.983
697.9798	Cr I 222	R	0.232	14.08	-5.293	0.998
698.0913	Cr I 222	B	0.056	10.81	-6.011	0.992

TABLE I *(continued)*.

Wavelength	Ident	Mode	D^L	FWHM	$\log(W/\lambda)^L$	F^L_L/F^{SP}_Φ
698.8529	Fe I	167 W	0.254	12.54	-5.292	0.998
699.6653	Ti I	256 B	0.018	9.93	-6.587	0.995

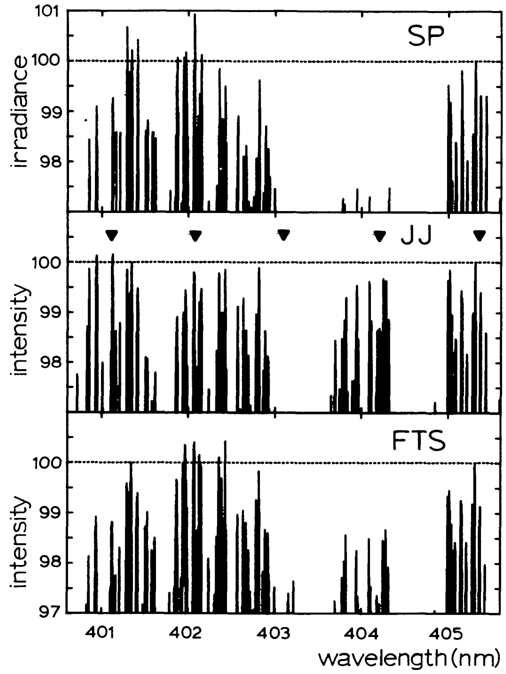

FIGURE 1. — Comparison of the background windows in the SP Atlas, in the JJ Atlas, and in KPNO-FTS data, for a short wavelength interval in the blue where these data sets overlap.

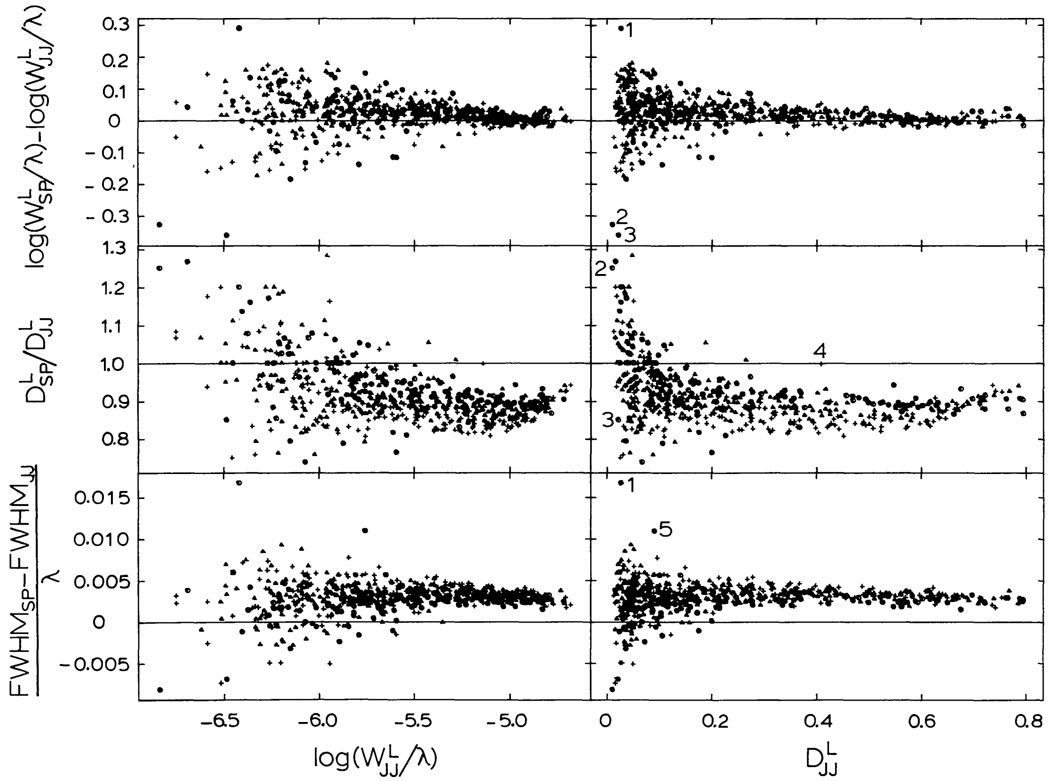

FIGURE 2. — Comparison of line-profile parameters measured from the SP Atlas and from the JJ Atlas for 602 clean lines. Horizontal : logarithmic line strengths from the JJ Atlas (left) ; line depths from the JJ Atlas (right). Vertical : difference in logarithmic line strengths (top) ; ratio of line depths (middle) ; difference in line halfwidths, normalized by the wavelength (bottom). All parameters are measured from the local continuum. Circles are lines from the wavelength interval $\lambda\lambda$400.6-500 nm, triangles from $\lambda\lambda$500-600 nm ; crosses from $\lambda\lambda$600-700 nm. (The numbers identify deviating lines, respectively : 1 = λ450.421, 2 = λ456.603, 3 = λ495.430, 4 = λ695.125 and 5 = λ441.339.)